Notes on Axial-Mode Helical Antennas in Amateur Service

L. B. Cebik, W4RNL
1434 High Mesa Drive
Knoxville, TN 37938-4443
e-mail: cebik@cebik.com

The axial-mode helical antenna has become a popular choice for radio amateurs engaging in satellite communications. We may construct helical antennas using straightforward methods with easily available materials. However, the individual builder faces a number of questions about helix size for a given frequency. Past literature has focused mainly on the gain that the axial-mode helix can attain for a given size. We should also examine other facets of the helix, such as the sensitivity to feedpoint impedance change with very small variations in size and the development of sidelobes with changing helix size.

In addition, the axial-mode helix generally receives attention in the context of very broadband antennas. In contrast, the amateur seeking circular polarization for satellite communications normally uses a very small bandwidth on any one of several bands, each band requiring a separate antenna. To answer the questions that face the potential amateur helix builder, we must we change our orientation to the antenna. Then we may be able to answer not only the question of how large to build the antenna, but as well whether the axial-mode helix is the right choice for a circularly polarized antenna for some specific use.

There are a number of background sources for information on axial-mode helices. The following list is a start, with most of the items having extensive bibliographies.

John D. Kraus, *Antennas*, 2nd Ed. (1988), pp. 300-310.
W. L. Stutzman and G. A. Thiele, *Antenna Theory and Design*, 2nd Ed. (1998), pp. 231-239.
C. A. Balanis, *Antenna Theory*, 2nd Ed. (1997), pp. 505-512.
H. E. King and J. L. Wong, "Helical Antennas," Chapter 13 of *Antenna Engineering Handbook*, 3rd Ed., R. L. Johnson, Ed. (1993), pp. 13-1 ff.
Darrel Emerson, AA4FV, "The Gain of an Axial-Mode Helix Antenna," *The ARRL Antenna Compendium*, Vol. 4 (1995), pp. 64-68.
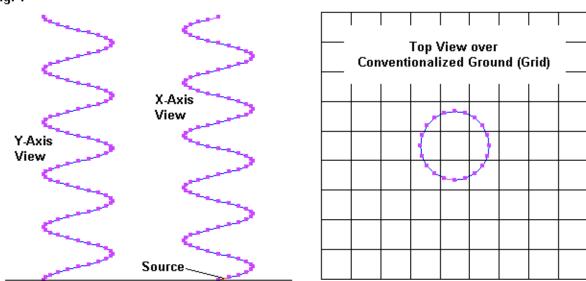
The fundamental question posed by virtually all of these sources is the gain of the helix relative to its proportions over a significant bandwidth. In the notes to follow, I shall purposely restrict the number of size considerations and also reduce the bandwidth to a single frequency: 299.7925 MHz. At this frequency, 1m = 1λ. Therefore, all measurements will be in meters. The properties of any sample helix will scale to any desired frequency so long as you also scale the wire diameter.

My investigation will use NEC-4D as the chief modeling tool. For most purposes, NEC-2 will also work, although the helix formation command has a different entry system for the critical dimensions. NEC results in the past have appeared to yield lower gain reports than some indirect gain calculations based on empirical results. However, there are both modeling and theoretical calculation issues related to the interpretation of the modeling reports, and we shall examine both before we are done.

Some Helical Antenna Basics

A typical axial-mode helical antenna has the form shown in **Fig. 1**. It consists of a number of turns, usually rising from a ground plane. The graphical representation of the helix shows the modeling form that I used to generate the basic sections of these notes. The bottom end of the helix connects directly to a perfect indefinitely large ground plane. Peak forward gain occurs close to or at the vertical axis of the helix. However, as we shall see, the pattern of a helix is not always perfectly symmetrical. There are numerous construction variations. Some builders bring the bottom turn of the helix back to the center of the helix circle. Others surround the base with a cup connected to the ground plane. Of course, an actual ground plane will have a finite dimension, usually a full wavelength in diameter or along the sides of a square.

Fig. 1

5-Turn Heical Antenna Over Perfect Ground

The helices with which we shall work are straight sided. King and Wong have worked with both stepped and uniformly tapering helix diameters, but most amateur builders will choose the simpler uniform structure shown in **Fig. 1**.
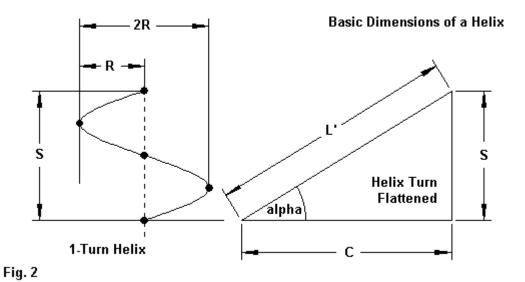

Fig. 2

Fig. 2 shows the basic dimensions of a helix. S is the turn spacing or the linear length of 1 turn of the helix. R is the radius, and 2R the diameter. If we stretch a single turn flat, we obtain the right triangle shown on the right side of the figure. C indicates the circumference of the turn, while L' indicates the length of wire required to obtain a full turn. Angle α is the pitch of the helix. For helices having multiple turns, we shall also be interested in the total helix length.

The dimensions are all interrelated by a few trig equations. All dimensions refer to center-to-center distances relative to the wires.

R = radius of the helix, wire-center to wire-center
C = circumference of the helix $\qquad$ C = 2 π R
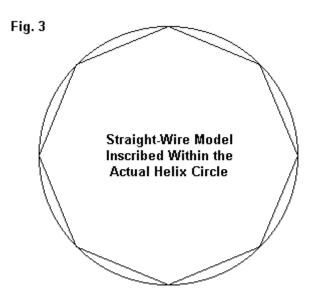S = spacing between turns $\qquad$ S = C tanα
α = pitch angle $\qquad$ α = tan^{-1} (S/C)
N (or n) = number of turns
L = axial length of helix $\qquad$ L = n S
D = conductor diameter
L' = Conductor length for a single turn $\qquad$ L' = SQRT(C^2 + S^2) = C/cosα = S/sinα

To design of an axial-mode helix, we need select only a few of these dimensions and the rest will following automatically. Perhaps the two most critical dimensions are the pitch angle and the circumference. In fact, basic helix theory tends to restrict axial-mode operation of the helix to pitch angles between 12° and 14°. As well, various texts restrict the circumference to ranges from either 0.8λ to 1.2λ (Kraus) or from 3/4λ to 4/3λ (Balanis). The number of turns in a helix is a builder selection, with gain (for any given pitch and circumference) rising with the number of turns. As well, selection of a wire diameter is also a builder choice. Although not mentioned in any serious way in most literature, we shall discover that the conductor size does make a difference to helix performance.

Modeling a helix in either NEC-2 or NEC-4 involves approximating a circular form with a series of straight wires. **Fig. 3** shows one limitation of this process. The straight-wire segments are inscribed within the circle defined by the specification of a radius for the helix. Hence, the sum of the wire segments will always be less than the length of the wire in an actual single turn. If we raise the number of segments sufficiently high, the error diminishes to insignificance. A level of about 20 wires per turn is large enough for virtually all applications.

Fig. 3

Straight-Wire Model
Inscribed Within the
Actual Helix Circle

Modeling Limitation for Helical Antennas

The following two lines compare otherwise identical 5-turn helices with a circumference of 1.0λ and a 12° pitch at the test frequency.

Segmentation Segments/turn	Reported Gain dBi	Impedance R +/- jX Ω	Average Gain Test		Corrected Gain dBi
			Value	dB	
20	8.39	225.5 - j 39.8	1.815	-0.42	8.81
40	8.30	213.2 - j 71.2	1.762	-0.55	8.85

Ultimately, the corrected gain values (reported gain - AGT in dB) coincide very well. However, given the model set-up, the impedance values (even if corrected by multiplying half the AGT value times the resistive component) will not coincide. To gather trends, but not actual values, of the terminal impedance of the helix, I placed the source on the very first segment. However, NEC places a source on the entire segment. Changing the number of segments per turn places the actual position of the source either closer to or further from the ground plane. Hence, the more segments per turn, the lower the resistive component of the source impedance.

The use of the first segment as a source position has a second effect on the model. A NEC model is most adequate when the segments on either side of the source are equal in length or when the source segment is vertically oriented to a perfect ground plane. The helix meets neither of these conditions. Hence, the average gain test (AGT) value for a helix over perfect ground is not 2.0. However, we may correct the reported gain value (in dBi) by subtracting the AGT value in dB from the reported value. The following lines compare the 5-turn 12° 1.0λ helix with the source placed on segments 1, 2, and 3.

Source Placement	Reported Gain dBi	Impedance R +/- jX Ω	Average Gain Test Value	dB	Corrected Gain dBi
Seg. 1	8.39	225.5 - j 39.8	1.815	-0.42	8.81
Seg. 2	8.79	238.2 + j 44.2	1.995	-0.01	8.80
Seg. 3	8.79	263.1 + j147.3	2.000	0.00	8.79

Using the AGT value to correct the gain figure is thus a completely effective means of arriving at the modeled helix gain. However, had we used the impedances at segments 2 or 3 instead of going through the process of correcting the model for its AGT value, we would not see the impedance trends as well at the terminal end of the structure. Although the reported values will still be off the mark by a distance roughly equal to half the length of a segment, they will still be adequate to let us examine trends. Because we only need to see trends, we do not need to correct the resistive component of these values, especially since this corrective becomes less secure with high values of reactance.

NEC-4 models of helices are deceptively simple, as the following sample reveals.

```
CM General Helix over Perfect Ground
CE
GH 1 100 5 1.24664 .159155 .159155 .001 .001 0
GE 1 -1 0
GN 1
EX 0 1 1 0 1 0
FR 0 1 0 0 299.7925 1
RP 0 181 1 1000 -90 90 1.00000 1.00000
RP 0 181 1 1000 -90 0 1.00000 1.00000
EN
```

The entire 100-segment model of the 5-turn helix is contained in the single GH entry. It specifies 100 segments in 5 turns with an overall length of 1.24664 m (λ) using a starting and ending radius of 0.159155 m (λ) with starting and ending wire radii of 0.001 m (or 1 mm). The remainder of the model specifies the test frequency (FR), the source position (EX), the perfect ground (GN), and the requests for 2 theta (elevation) patterns at 90° phi (azimuth) angles from each other. The 2 patterns allow us to see the slight non-symmetry of the helix pattern over a perfect ground. (We shall examine the usual NEC-2 version of the GH command before we conclude these notes.) It is possible to create a helix using individual wires, and some programs include, either as part of the program or as an adjunct program, methods of creating helices. However, these systems will produce individual wires for each segment of the helix. Using the GH command, the NEC core calculates and produces the required segments internally. The ability to change the size of a helix with only a few keystrokes allows a larger database in a shorter time. However, before we conclude these notes, we shall change techniques, since rapid methods of helix formation also have their limitations.

There is such a thing as presenting too much data in compressed form for effective absorption. Many of the engineering charts developed for axial-mode helices suffer from this syndrome. Therefore, I shall restrict my investigation in several ways. First, I shall use (except for a single demonstration) a constant wire diameter of 2 mm (0.002λ or about 0.07874"). Second, I shall restrict the pitch angles to 14° and 12° (again, except for a single demonstration). These pitches represent the limits recommended for axial-mode helix operation and suffice to show trends based upon changing the pitch. Third, I shall look at helixes using 5, 10, and 15 turns only, since these represent short, medium, and long antennas. Most reference books place a lower limit of about 4 turns for axial-mode operation, so the shortest helix in our batch is close to the limit. 15 turns can result in helices up to 5λ long. Finally, we shall examine changes in performance of the prescribed helices using circumferences from 0.75λ up to 1.35λ. Extending the circumference to the Balanis 3/4λ-4/3λ limits lets us view some properties of these antennas that we might otherwise overlook. Because wire losses are so small in a helix, we shall use perfect (lossless) wire throughout. Let's begin with the smallest of our samples.

A 5-Turn Helix Using 2-mm Diameter Wire

The first test model is a 5-turn helix that uses 2-mm diameter lossless wire. The initial test used 4 separate pitches: 14°, 12°, 10° and 8°. For any small circumference, the gain increases as the pitch diminishes (and with it, the turn spacing and the total length). I wanted to uncover what the consequences might be of extending each pitch through larger circumferences. 14° is the recommended maximum pitch angle. The minimum circumference in the survey is 0.75λ. The maximum circumference is generally 1.35λ, although one data table uses 1.4λ as the maximum to confirm that the gain begins to drop beyond 1.35λ.

Table 1 shows the numerical data for the 4 series of modeling runs. The table derives from a simple spreadsheet used to calculate the required dimensions for the models. "Circum" means the helix circumference, while "Radius" is self-explanatory and is calculated by the spreadsheet. My spreadsheet actually uses 16 numeric positions per calculated number, although the table shows only 8. The extra positions are more of an inconvenience to data copying than they are an aid to precision. "T-space" means the turn spacing, again, as calculated from the pitch angle and the circumference. "Length" is the total length of the antenna, in this case 5 turns times the turn spacing.

Recorded data begins with "Gain Rp," the reported gain from the initial modeling. "BW-90" is the beamwidth as viewed down the Y-axis, while "BW-0" is the beamwidth down the X-axis, where beamwidth for both is the -3dB value. "R" and "X" are the components of the source impedance in Ohms. "AGT #" is the calculated average gain test value over perfect ground, where a value of 2.0 represents a fully adequate model as measured by this test. (Note that AGT is a necessary but not a sufficient condition of model adequacy.) "AGT-dB" is the same value converted to dB to serve as a correction factor for the reported gain. When calculated over perfect ground, use half the value of the report AGT, take the $\log_{10}$ of that number, and multiply by 10 to arrive at the AGT-dB value. Since both values are rounded, a digit of deviance is possible. The final or "Gain-Cor" column gives the adjusted forward gain value by subtracting the AGT-dB value from the reported gain value. Since all AGT-dB values in these notes are negative, all corrected gain values will be higher than the reported values.

AGT values will vary slightly from one model in a series to the next and, as a block, from one set of runs to the next. The chief source of the low AGT value is the relationship of the source segment to the ground plane. This relationship changes slightly with every increase in circumference, since the source segment becomes slightly longer. As we change pitch to a smaller angle, the source segments again change their relationship to the ground plane. Hence, the AGT # and AGT-dB values both tend to decrease as the pitch becomes smaller.

Scanning the tables for patterns can be somewhat daunting, so I have graphed some of the key values, beginning with the maximum forward gain--using corrected gain values. The trends would not have changed had I used the initially reported values.
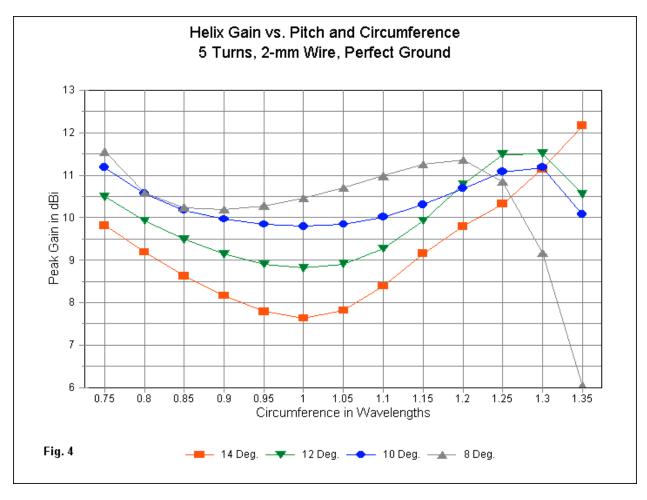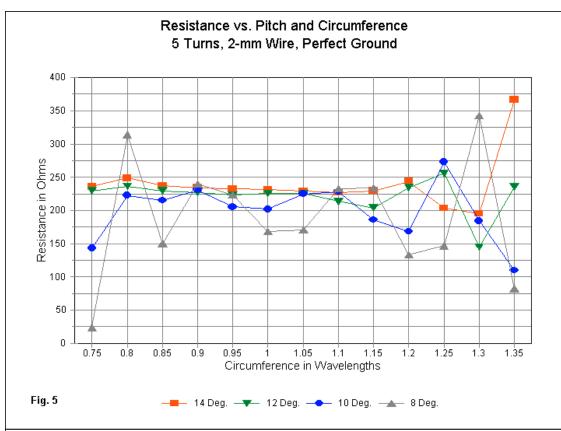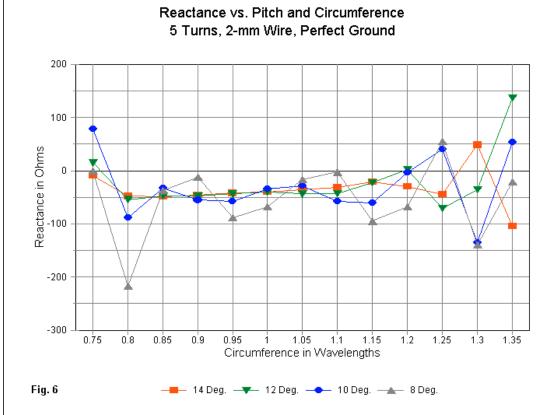
Helix Gain vs. Pitch and Circumference
5 Turns, 2-mm Wire, Perfect Ground

Fig. 4

Legend: 14 Deg. — 12 Deg. — 10 Deg. — 8 Deg.

Fig. 4 shows the maximum forward (upward) gains for the 4 pitch angles as we increase the circumference from 0.75 to 1.35λ. (The table shows the 14° 1.4λ circumference value to verify that the 1.35λ circumference value on the graph is a maximum that falls off with a larger circumference.) The trend in the gain graph suggests that we would do well with any of the 4 pitches up through a circumference of about 1.2λ. The lower the pitch, the higher the gain we obtain for any circumference below 1.2λ. It is most interesting that the gain is lowest (for the 12° and 14° pitch angles) where the circumference is close to 1.0λ. Note, however, that as we reduce the pitch angle, minimum gain tends to become associated with smaller circumferences. If we were to move either upward or downward from the design frequency, any circumference (and radius) of choice would change with the new frequency. Therefore, the curves represent a tracking of the gain at frequencies some distance from the design frequency. The 0.75λ and 1.35λ cut-off circumferences limit the tracking to a corresponding frequency range relative to the test frequency.
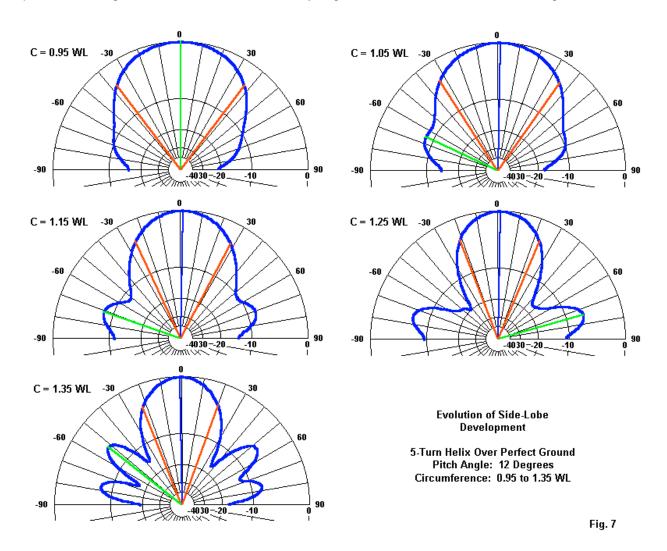
The gain curves do not tell the entire story concerning helical antennas operated in the axial mode. For example, one desirable feature of an antenna that we might wish to build is that all of the key properties should remain stable and predictable over a generous frequency span. We do not need them to be unchanging so long as we can easily predict the direction and amount of change. Small physical changes that yield large changes in a performance property tend to result in an antenna that is difficult to replicate within the tolerances of the usual home shop.

For this reason, graphs of the resistive and reactive components of the source impedance become important. **Fig. 5** and **Fig. 6** present the data for the 4 pitches relative to the 5-turn helix. Although the precise values are subject to adjustment as terminal impedance values, the trends may show us something of the helical antenna's stability.

Fig. 5

Resistance vs. Pitch and Circumference
5 Turns, 2-mm Wire, Perfect Ground

Legend: 14 Deg. | 12 Deg. | 10 Deg. | 8 Deg.

Fig. 6

Reactance vs. Pitch and Circumference
5 Turns, 2-mm Wire, Perfect Ground

Legend: 14 Deg. | 12 Deg. | 10 Deg. | 8 Deg.

Both the resistance and the reactance curves for the 10° and the 8° curves show significant fluctuations at virtually any circumference of helix, especially as compared to the 14° and the 12° curves. Even these curves have their limits. Above about a 1.2λ circumference, the high-pitch curves show very significant fluctuations. Reactance swings of 70Ω are common with a circumference change of as little as 0.05λ. For the 5-turn helix, 14° and 12° pitch helices less than 1.2λ long appear to present the most stable designs with respect to source impedance. Circumferences below about 0.8λ for 12° and 14° pitches also begin to show the instabilities of very large circumferences, but to a lesser degree.

Evolution of Side-Lobe Development

5-Turn Helix Over Perfect Ground
Pitch Angle: 12 Degrees
Circumference: 0.95 to 1.35 WL

Fig. 7

A second factor often overlooked in helix performance is the development of sidelobes. **Fig. 7** shows the Y-axis elevation patterns of the 5-turn helix with a 12° pitch over stepped circumferences. Although the sidelobes at circumferences of 1.05λ and 1.15λ appear small, note that they are less than 10 dB below the level of the maximum forward gain. As we increase the circumference, the sidelobes become stronger, and by a circumference of 1.35λ, we have a double set, with the forward-most sidelobe only about 6 dB below the main lobe. At the low end of the circumference scale, patterns for sizes below 0.95λ tend to remain as well behaved as the first pattern in **Fig. 7**.

Another feature of the helix's sidelobe development is the fact that neither the main lobe nor the sidelobes are symmetrical with respect to the centerline. Even the 1.05λ circumference pattern shows the asymmetry. In fact, the patterns are more symmetrical as viewed along the Y-axis than along the X-axis. If you return to **Fig. 1**, you can see that the terminal end of the model is off center when viewed along the Y-axis. The result is larger secondary lobes on one side than the other side of the helix.

The sidelobe development, when added to the source impedance data, suggests that in many ways, we would derive better performance overall from a 5-turn helix with a circumference above 0.8λ and under 1.2λ. This practical restriction lowers the maximum gain that we may obtain from the antenna to under 10 dBi with a beamwidth of about 50 degrees or so.

At this point, we must wonder if the same trends hold up for 10-turn and 15-turn helices. However, before examining that data, let's examine another overlooked aspect of helix design.

A 5-Turn Helix Using 5-mm Diameter Wire

Let's increase the wire diameter from 2 mm to 5 mm. 2-mm wire is between AWG #12 and AWG #14 in diameter. 5-mm wire is about 0.1969" in diameter, a little larger than 3/16" rod. At 2.5 times the diameter of our first models, it represents a way to discover whether element diameter makes a difference to helix performance.

One limitation of the investigation is the fact that the AGT values continue to drop further below the ideal 2.0 value. Nevertheless, the data are sufficiently accurate to reveal trends as we run through 14° and 12° pitch 5-turn helices. **Table 2** has the complete data, but a few graphs can focus our attention on a number of key factors.
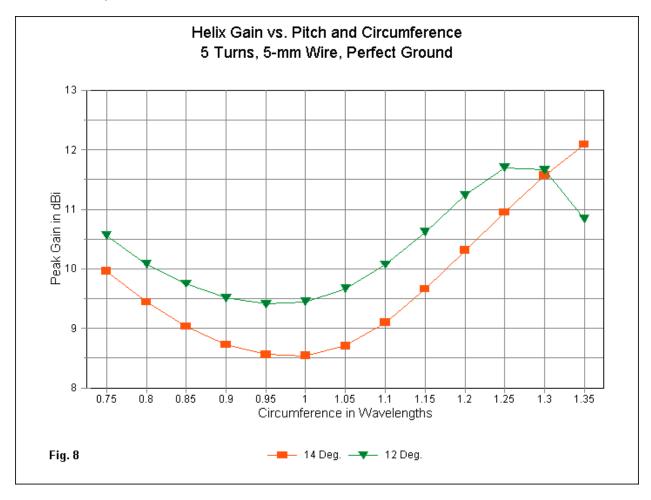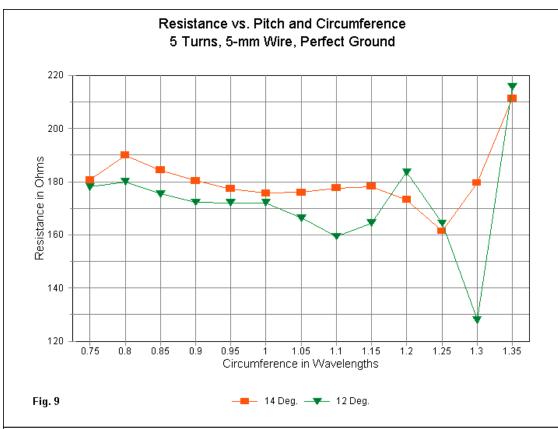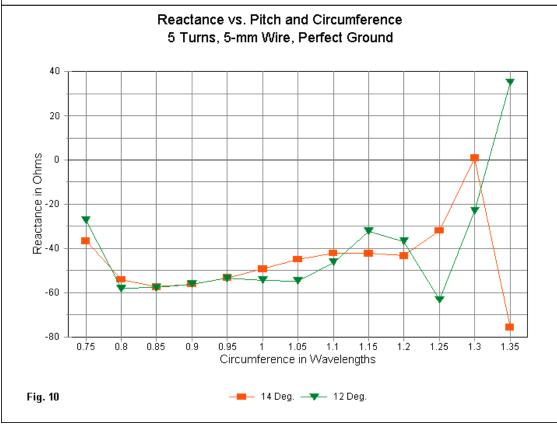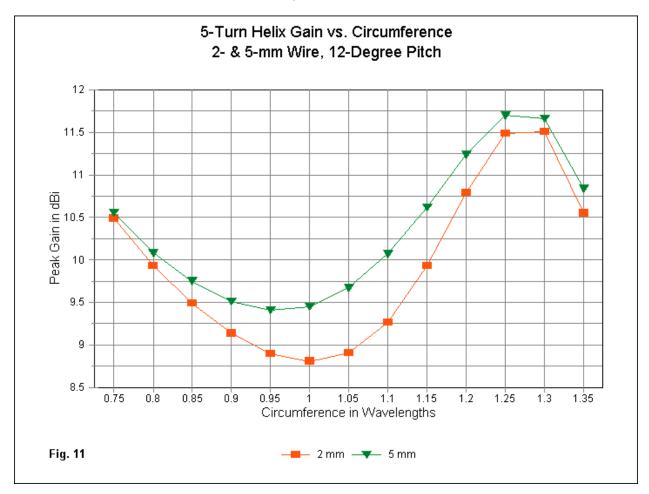

Fig. 8

Fig. 8 presents the gain data for the two subject models for the standard range of circumferences. Both curves closely parallel their counterpart curves for 2-mm wire. The tabular data for 1.4λ will confirm that the 1.35λ gain for the 14° curve is a peak value.

Fig. 9

Resistance vs. Pitch and Circumference
5 Turns, 5-mm Wire, Perfect Ground

Fig. 10

Reactance vs. Pitch and Circumference
5 Turns, 5-mm Wire, Perfect Ground

In **Fig. 9** and **Fig. 10** we can see the instabilities of the resistance and reactance performance for circumferences below about 0.85λ and above 1.2λ. However, should we wish to compare the curves for smaller circumferences with the corresponding 2-mm curves, we shall see similar variations (and similar stability) for the two wire sizes. (Note: differences in the Y-axis range on the graphs may leave a misimpression of the actual amount of change.) In general, then, wire size does not make a great deal of difference to the selection of a helix circumference. Indeed, the patterns for the 5-mm helices are too close to those for the 2-mm versions to need repetition.

Fig. 11

Wire diameter does make a difference in the forward gain of a 5-turn helix, especially over the range of circumferences that we have so far listed as stable with respect to source impedance and relatively free of sidelobe development, that is, 0.85λ up to about 1.2λ. **Fig. 11** shows gain curves for the two wire sizes using a 12° pitch. Note that, besides gain, the only notable feature is the circumference associated with the minimum gain value. The movement of that gain "null" is similar to the effect of reducing the pitch angle with a constant wire size. (See **Fig. 4**.) Inter-turn coupling thus becomes a possibility for explaining the movement of the gain-null circumference size.

Within the "stable" range, the average gain advantage for 5-mm wire is about 0.5 dB. The largest differences occur with circumference sizes between about 0.95λ and 1.15λ. Although one may dispute just how much advantage a half dB makes operationally, the result does have a bearing on most of the methods for estimating axial-mode helical antenna gain. None of those techniques takes wire diameter into account. In applying this data to scaled versions of the helices under study, we should remember that 2 mm and 5 mm represent 0.002λ and 0.005λ wire diameters, respectively.

A 10-Turn Helix Using 2-mm Diameter Wire

A 5-turn helix is just barely larger than the 4-turn limit for the application of axial-mode theory to antenna performance. Doubling that length to 10 turns yields a middle-size antenna, perhaps long for the amateur 2-meter band, but still shorter than those in use at 1296 MHz. Using 2-mm diameter wire and restricting ourselves to pitches of 14° and 12°, we obtain helical antennas that vary from 1.6λ to almost 3.4λ in total length. Our primary question will be whether there are any changes in the characteristics of these antennas other than the anticipated increase in maximum gain.

Table 3 provides the modeling data for the series of 10-turn helices. The overall increase in gain is accompanied by an equally expected reduction in beamwidth as we compare data for each level of circumference. However, for the smaller circumferences, the source impedance does not change by any very significant amount, a fact that is consistent with established helix theory and measurement. As well, for this modeling investigation, the AGT values for both helix lengths are consistent with each other.
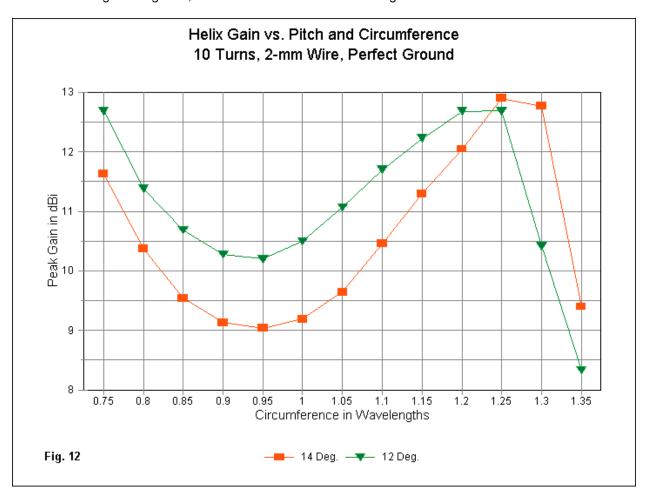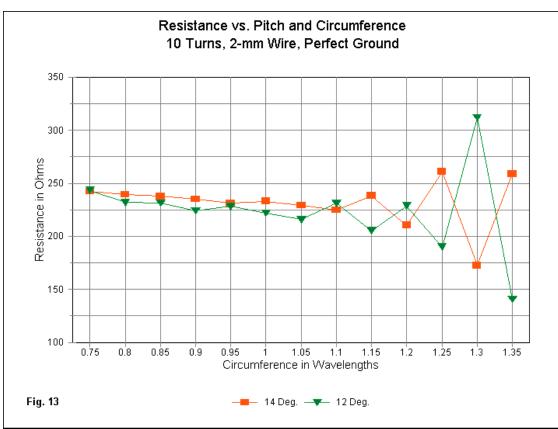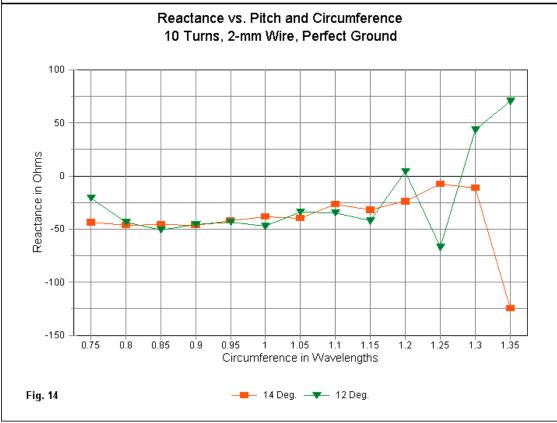

Fig. 12

Fig. 12 presents the gain data for the range of circumference covered by this study. Note that, compared with the 5-turn helices, both pitch versions reach their peak gain values at circumferences about 0.1λ smaller. The 12°-pitch version reaches peak gain at a circumference of about 1.2λ. Small-circumference gain values approach the peak gains of large-circumference versions. However, we suspect in advance that the usable region of the curves is smaller than the total span. As well, the minimum gain values occur at about 0.95λ circumference levels. The tilt of the curves in this area suggests that the actual minimum value for the 12° curve occurs with a slightly smaller circumference than for the 14° model.

Fig. 13

Resistance vs. Pitch and Circumference
10 Turns, 2-mm Wire, Perfect Ground

Fig. 14

Reactance vs. Pitch and Circumference
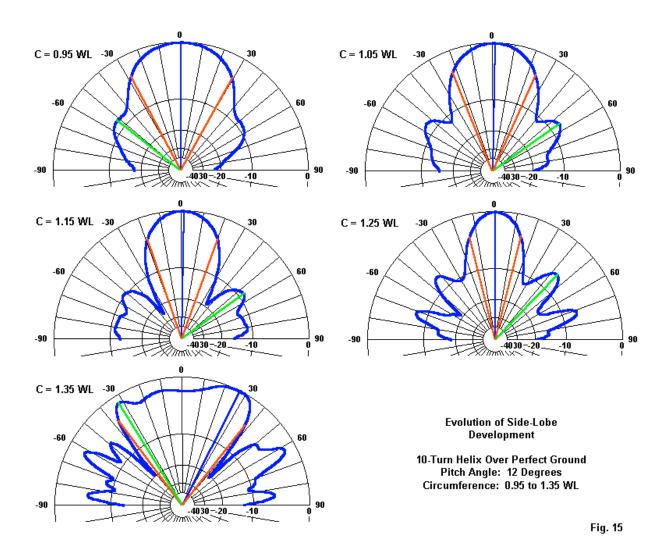10 Turns, 2-mm Wire, Perfect Ground

The source resistance and reactance data also show some degree of stability shift toward the smaller circumference values. The 12°-pitch version of the helix begins to show wider variations of both resistance and reactance at a circumference of about 1.15λ. The lower gain 14°-pitch model appears stable with respect to reactance to about 1.2λ, but the resistance begins to show instabilities just shy of that circumference. These trends appear in **Fig. 13** and **Fig. 14**. At the low end of the scale, instabilities begin to appear only for the smallest circumference within the survey.

The end result is that the 10-turn helix appears to be stable to almost the same circumference as the 5-turn helix when we restrict ourselves to 14° and 12° pitch levels. At most, we shrink the stability limit by one step, down to a circumference of 1.15λ.

We are as interested in pattern shapes as we are in other performance factors. Here, **Fig. 15** can be useful, as it presents the Y-axis elevation patterns for the 12° pitch 10-turn helix at the same circumferences used in **Fig. 7**. The patterns make several things clear. First, past the gain peak, a 10-turn helix is quite unsatisfactory as an axial mode antenna. In fact, the single dome pattern reappears at various larger circumferences, but it has lost the consistency that marks axial mode operation.

Evolution of Side-Lobe
Development

10-Turn Helix Over Perfect Ground
Pitch Angle: 12 Degrees
Circumference: 0.95 to 1.35 WL

Fig. 15

Second, just as the gain peaked at a smaller circumference than for the 5-turn antenna, the sidelobes begin their appearance at a smaller circumference in 10-turn antennas. The sidelobes of the 10-turn helix
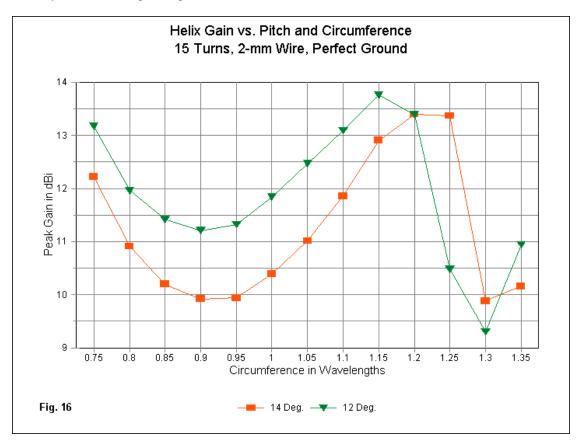
with a 0.95λ circumference are nearly as distinct as the ones that we encounter in the 5-turn helix only at a circumference of about 1.15λ.

Third, the sidelobe structure becomes more complex, even if we restrict our attention to patterns for circumferences up to 1.15λ. Rather than having single or double side lobes, we have a wider sidelobe that suggests the inclusion of several overlapping sidelobes. Although the peak values are not as high as in the case of some 5-turn patterns, the total energy within the sidelobes may be equal to single stronger lobes. In terms of the pick-up of unwanted noise and signals in directions other than the focus of the main lobe, the effects may be similar.
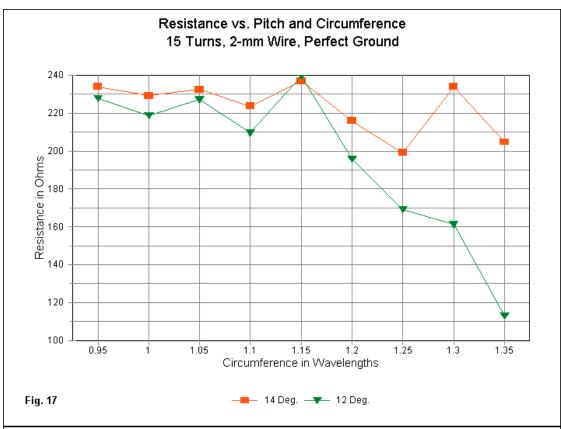
Whether the trends continue or whether the helices have stabilized requires one more set or models.
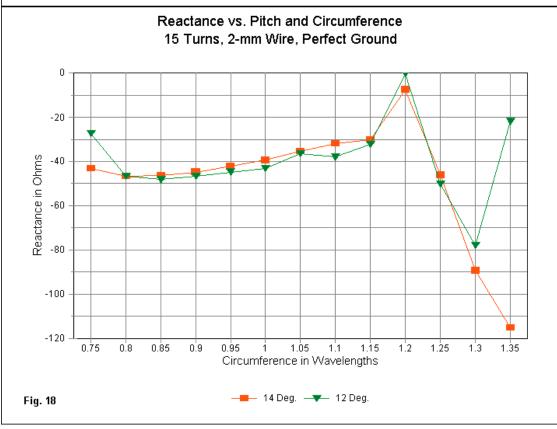
A 15-Turn Helix Using 2-mm Diameter Wire

At the design frequency, 15-turn axial-mode helices with circumferences between 0.75λ and 1.35λ yield antennas between 2.4λ and 5.0λ long. We may generally classify these antennas as long helices. Longer helical antennas are possible, but these would be quite rare in amateur service. The long antennas yield their anticipated further increase in gain along with the accompanying decrease in beamwidth. Despite the increased length, the long helices do not yield perfectly aligned patterns, as evidenced by the continuing divergence between X-axis and Y-axis beamwidth data in **Table 4**.

Fig. 16

The gain data captured in **Fig. 16** shows a further compression of the gain curve toward the smaller circumferences. The gain peaks are at least one step smaller in circumference, with more precipitous declines in gain above the circumference of peak gain. Even if we press the circumference for maximum gain, the limit of utility is well below the maximum circumference (about 1.3λ) for which axial-mode helical antenna theory is most often rated.

Resistance vs. Pitch and Circumference
15 Turns, 2-mm Wire, Perfect Ground

Fig. 17

Reactance vs. Pitch and Circumference
15 Turns, 2-mm Wire, Perfect Ground

Fig. 18

The 15-turn source impedance data also suggest that circumferences below 1.15λ are best suited for stable operation, as shown in **Fig. 17** and **Fig. 18**. With respect to source resistance, the 14° version is more stable. The variations in the 12°-pitch version are not an artifact of modeling, since the AGT values of the 15-turn helices are comparable to those of the 5-turn and 10-turn antennas for each pitch shown. However, it is notable that the region of relatively stable resistance values continues to move toward small circumferences.

Although the resistance of the 14° model shows the greater stability, reactance is the opposite. With respect to reactance, the 12° version shows greater stability, but not by much. At the upper end of the circumference scale, both pitches show radically divergent values with respect to the stable region, suggesting that the longer the axial-mode helix, the more that circumference limits represent a sudden threshold rather than a gradual transition into unreliable operation.

The net result of the data is the suggestion that the home builder of a long helix should use great care if he wishes to press the limits of gain and source impedance at the 15-turn level. Construction variables may easily push the antenna over the limits of stable performance. Conservative design using smaller circumference values may make the resulting antenna easier to tame than versions using large values for the circumference.

Evolution of Side-Lobe
Development

15-Turn Helix Over Perfect Ground
Pitch Angle: 12 Degrees
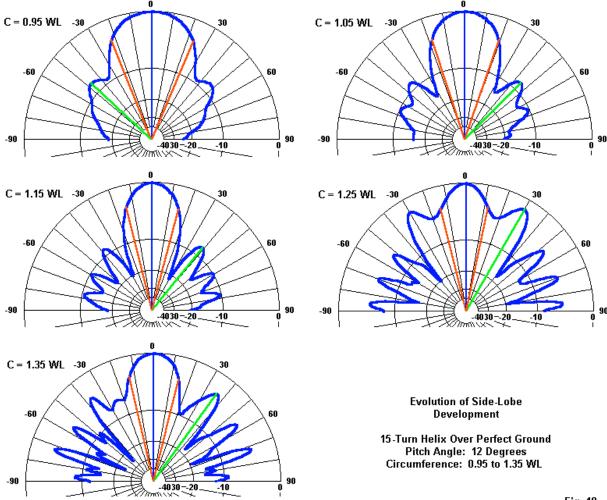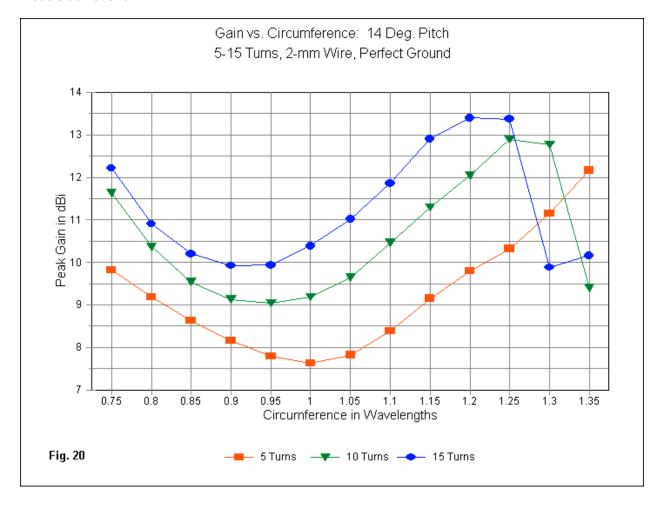Circumference: 0.95 to 1.35 WL

Fig. 19

The trends in pattern formation that we have observed through the 5-turn and 10-turn helices continue in the longer version. Sidelobes development occurs at smaller circumferences, with a definitive
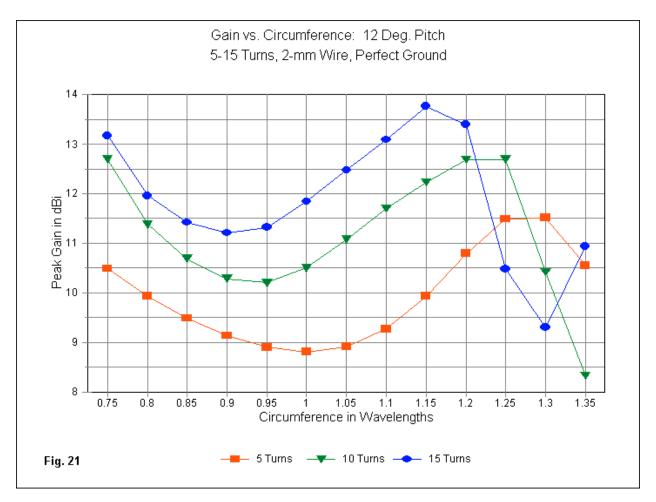
and an incipient sidelobe already apparent in the pattern in **Fig. 19** for a circumference of 0.95λ. The pattern is relatively free of side lobes only at the smallest circumferences surveyed in these notes. Only the patterns through a circumference of 1.15λ are suitable for axial-mode operation. (Note from the pattern for a circumference of 1.25λ that a narrow half-power beamwidth does not clearly indicate a desirable axial-mode pattern.) Even with single central forward lobes, the sidelobes of the long helices should be a matter of concern, since they are down from the main lobe by less than 10 dB in these models using a perfect ground as the modeling ground plane.

Some Comparisons

    To summarize part of what the data show, we may compare the gain curves for both the 14° and the 12° versions of the three levels of helices studied here. **Fig. 20** compares the gain curves for the 14° antennas, while **Fig. 21** does the same for the 12° models. For both pitches, note that there is strong parallel among the three curves. However, the longer the helix, the greater is the displacement of the curve toward the smaller values of circumference.

    Equally apparent is the parallelism among curves with respect to the gain decrease above the peak gain point. As the pattern graphics have shown, operation above the peak gain level yields generally unsatisfactory axial-mode radiation patterns, not to mention operation in regions of unstable source resistance and reactance values. How far one may push the circumference smaller than the limit shown on the graph to capitalize on a clean pattern and higher gain on this side of the main minimum would require further study. However, in terms of real helices using a self-contained ground plane and positioned some distance above the actual ground, there will be limitations that the perfect-ground models do not show.

Fig. 20

Gain vs. Circumference: 12 Deg. Pitch
5-15 Turns, 2-mm Wire, Perfect Ground

Fig. 21   ■ 5 Turns   ▼ 10 Turns   ● 15 Turns

We may also compare the gain values derived from this exploration with at least a couple of the shirt-pocket estimation schemes proposed in basic literature about axial-mode helical antennas. Similar calculation systems for gain and the half-power beamwidth appear in Kraus (p. 310) and in Stutzman and Thiele (p. 237). The terms for these calculations have the following meanings. C_λ = Circumference of helix in λ. S_λ = Turn spacing of helix in λ. n = number of turns in helix. λ = wavelength(s)

1. Gain (Directivity): Kraus
$D = 12\ C_\lambda^2\ n\ S_\lambda$

Stutzman & Thiele
$D = 6.2\ C_\lambda^2\ n\ S_\lambda$

Note: Gain (dBi) = $10 \log_{10}(D)$

2. -3dB (half-power) Beamwidth: Kraus
$HPBW = 52°/(C_\lambda\ SQRT(n\ S_\lambda))$

Stutzman & Thiele
$HPBW = 65°/(C_\lambda\ SQRT(n\ S_\lambda))$

3. Terminal Resistance: $R = 140\ C_\lambda$

$R = 140\ C_\lambda$

The original coefficient for directivity in Kraus was 15, but he had reduced this number to 12 by the release of the 2nd edition of *Antennas*. Although the equation for terminal resistance equation is common to virtually all systems, we shall not try to evaluate it, since the source values for a NEC model do not occur at the true terminal point of a helix.

As a test case, let's examine the data for helices with a 1.15λ circumference (using 2-mm wire) and compare the modeled values for 5-, 10-, and 15-turn versions. Gain is in dBi and BW (half-power beamwidth) is in degrees. Modeled data also appear for the 5-turn, 5-mm wire helix.

Turns	$L_\lambda = n\, S_\lambda$	Modeled		Kraus			Stutzman & Thiele		
		Gain	BW	D	Gain	BW	D	Gain	BW
5	1.222λ	9.93	53	16.9	12.3	41	8.7	9.4	51
5 (5-mm)	1.222λ	10.62	53						
10	2.444λ	12.23	39	33.7	15.3	29	17.4	12.4	36
15	3.666λ	13.76	28	50.6	17.0	24	26.1	14.2	26

As a second test case, let's evaluate helices with 0.85λ circumferences in the same manner.

Turns	$L_\lambda = n\, S_\lambda$	Modeled		Kraus			Stutzman & Thiele		
		Gain	BW	D	Gain	BW	D	Gain	BW
5	0.903λ	9.49	71	9.2	9.6	58	4.8	6.8	76
5 (5-mm)	0.903λ	9.75	69						
10	1.807λ	10.69	58	18.4	12.7	46	9.1	9.8	57
15	2.710λ	11.42	50	37.2	14.4	27	14.2	11.6	47

The calculating schemes can grow to into fairly complex affairs, as is evident in the more elaborate equations found in the Emerson and the King and Wong references. However, none take the wire radius (or diameter) into account. Hence, all remain shirt-pocket estimators and not precise calculators of the properties of axial-mode helical antennas, at least as modeled in this study. For practical purposes, that is, initial planning and the like, the Stutzman and Thiele simple formulas are as good as any. However, they remain seriously off the mark for shorter helices with smaller circumferences that fall on the curve below the gain minimum. The two simpler schemes presume a steadily rising gain across the span of allowed axial-mode circumferences, and that presumption is not correct with respect to the models surveyed here..

This exercise has used NEC-4 to produce the modeled results. NEC-2 also has a helix command, although its structure is quite different from the one used in NEC-4. The GH command does not appear in the original NEC-2 manual (NOSC TD 116, Vol. 2), but does appear in numerous implementations of NEC-2. The only significant difference between the model that we showed for NEC-4 and the NEC-2 counterpart appears in the GH entry in the following sample. (The GE entry also has a slight difference between the NEC-2 and NEC-4 versions.)

```
CM  NEC-2 GH helical antenna over perfect ground
CE
GH 1 100 .249328 1.24664 .159155 .159155 .159155 .159155 .001
GE 1
GN 1
EX 0 1 1 00 1 0
FR 0 1 0 0 299.7925 1
RP 0 181 1 1000 -90 90 1.00000 1.00000
RP 0 181 1 1000 -90 0 1.00000 1.00000
EN
```

Fig. 22 shows GNEC and NEC-Win Pro help screens for the GH entry to aid in explaining the differences. Whereas the NEC-4 entry uses the number of turns and the total helix length to internally calculate the turn spacing, the NEC-2 version uses the turn spacing and total length to calculate the number of turns. NEC-4 uses a single helix radius (at both top and bottom), but NEC-2 requires entries of radius for both X- and Y-axes to allow for oval spirals. Restricting the helix to a circular form in NEC-4 opens a floating decimal position that permits one to choose between log spirals and Archimedes spirals, which yield a difference in the turn positions only if the radii differ at the top and bottom of the spiral.

Fig. 22

The GH command in both systems yields a wire segment structure that runs from Z=0 to a Z-value that equals the total length of the helix. The circumference of the helix is centered at X=0 and Y=0. In both systems, the modeler must use the GM command to change the position or orientation of the helix, a maneuver that we have not yet needed for this exercise.

The key question is whether we can expect any significant differences in the reported output between NEC-2 and NEC-4. **Table 5** provides a negative answer with respect to 5-turn helices using 2-mm diameter wire for pitches of 14° and 12°. (The table repeats the data from **Table 1** to facilitate the comparison.) I ran the series using the sample model shown and with the additional EK (extended thin-wire kernel) command that is useful in NEC-2 when the segment length begins to approach the wire diameter. The EK command made no difference to the data output. This test also confirms that the chief source of low AGT values is the position of the source and the orientation of the wire segment on which it is placed. The bottom line is simply that NEC-2 is fully adequate for modeling axial-mode helices so long as the modeler uses the AGT value to correct the gain reports and recognizes the limitation inherent in the source impedance report.

Elevated Self-Contained Ground Planes

The notes that we have examined so far present an idealized portrait of the axial-mode helix. Gain curves are smooth over the region that we have termed "stable." Within that region, the modeled values of source impedance have also varied within quite small limits. With the stepped increases in helix length, the patterns have shown a progressive development, especially with respect to sidelobe production.

However, the helical antennas that amateurs and others build do not have the benefit of a perfectly reflecting ground plane that is indefinitely large. Instead, in accord with the general outlines of **Fig. 23**, they appear on self-contained ground planes of finite size with the entire array placed above ground by an amount determined by operational needs and practical feasibility.

10-Turn Helix
with Wire-Grid
Ground Plane

Helix 20 Segments
per Turn, 10 Turns,
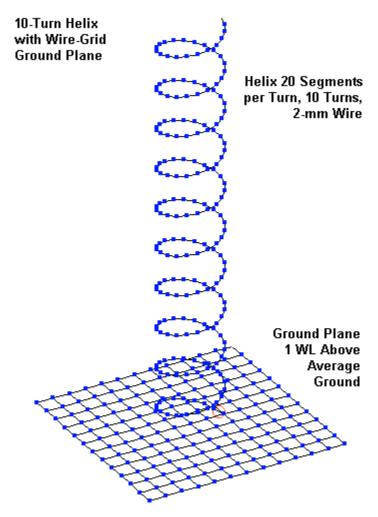2-mm Wire

Ground Plane
1 WL Above
Average
Ground

Fig. 23

As noted near the beginning of these notes, a square ground plane is not the only possible helical antenna configuration. However, from the perspective of practical modeling, it is perhaps the most appropriate for initial modeling efforts. As shown in the graphic, we may terminate the helical portion of the model at the nearest intersection of wires making up the wire-grid ground plane. Hence, the source may remain on the very first segment of the helix itself. The technique holds the promise of allowing some comparisons between the models constructed over perfect ground and the new series of models.

The new models do not come without an associated cost. The models over perfect ground made use of the GH command that permitted very simple model structures. However, if we use the same circumference steps with the new series of models, we need to move the terminal point of the first helix segment from its natural location to the nearest junction of ground-plane wires. We cannot do that and still keep the models simple and uniform from one step to the next.

The workaround for this problem is to construct individual models for each helix-wire-grid combination. As note at the beginning of these notes, several programs are available to allow the construction of both parts of the antenna on a 1-wire-per-segment basis. For example, EZNEC Pro/4's current version has both facilities. The resulting models are not any more segment intensive than using the GH and GM commands to create and replicate wires under a single tag number. However, they do result in one-model-per-situation. Hence, instead of using 1 model for all 12° antennas, we have one model for each combination of helix pitch, circumference, and length, plus the selected size of wire-grid ground plane.
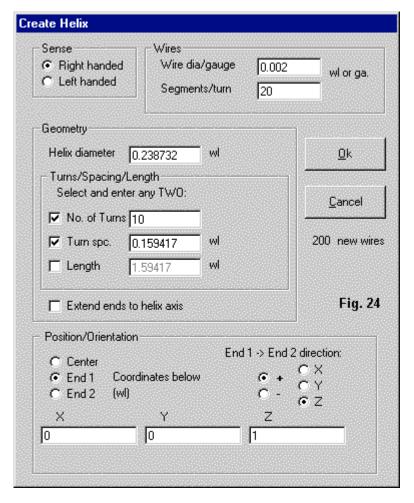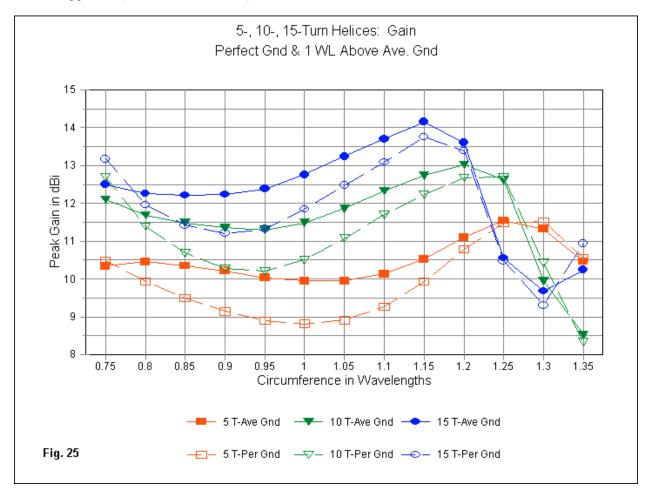

Fig. 24

Fig. 24 shows the EZNEC helix-creation sub-screen. Essentially, it allows entering the same set of variables as the GH command in either NEC-2 or NEC-4. However, the output is a set of 200 wires, each a GW entry. The wire-grid structure for this exercise is 1.2λ by 1.2λ on a side, with the wires spaced at 0.1λ intervals. Wire 1 of the helix shifts from its position on the X-axis as created to the nearest intersection of wires, normally either X=0.1 or X=0.2.
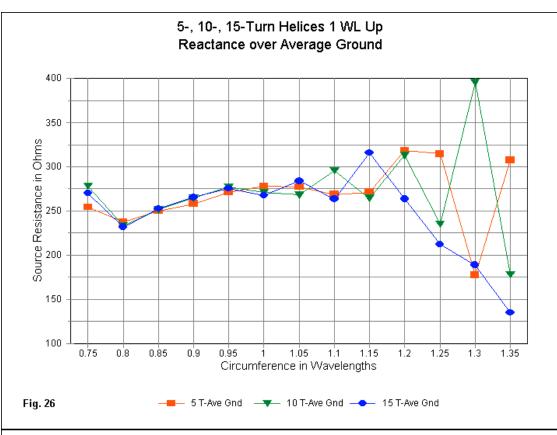
The models are limited by the factors that go into their creation. For example, the misalignment of the first helix wire creates a very small error component. More serious is the fact that the helix wire approaches the wire-grid wires at a severe angle: 12°. The normal wire diameter for a wire-grid that

simulates a solid surface is the segment length divided by π. However, this fat a wire results in some larger-circumference models having a first wire that penetrates into the center section of the wire-grid wire that it meets at a junction. To overcome this problem, I reduced the wire-grid diameters to 0.015λ. Although not a perfect simulation of a solid plane, the resulting data was--for models that could handle both thin and thick wires--only a slight change in performance.

Due to these constraints, I created models only for the 12° versions of the helical antennas, using 5, 10, and 15 turns, with radii ranging from 0.75λ to 1.35λ. Each helix connects to a wire-grid that is 1λ above average ground (conductivity 0.005 S/m, permittivity 13). The goal is to determine to what degree these models may differ from the models created over a perfect ground. **Table 6** provides the complete data on the modeling results. The AGT values tends to vary much more widely in these elevated ground-plane models than in the earlier set, but the values remain well within the range of what is usable to obtain suggestive (rather than definitive) trends.

Fig. 25

The general utility of the models shows up in **Fig. 25**, which tracks of gain levels for both types of models. Over the region that we termed "stable" with the initial set of models, the new models show identical characteristics, with a gain minimum occurring very close to where it occurred over perfect ground. As well, once the models use circumferences that place them outside of effective axial-mode use, the curves overlap fairly precisely. At the small-circumference end of the scale, the new models show lower gain than their perfect-ground counterparts as the circumference reaches a value too small for axial-mode duty. Within the more central portions of the circumference rage, the two curves for each length of helix parallel each other. The two differences are 1. the elevated models have a higher average gain than the perfect-ground models, and 2. the elevated models show a less severe dip in gain at the minimum point.
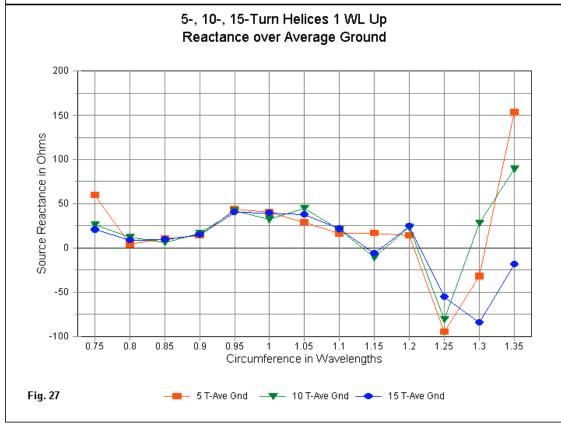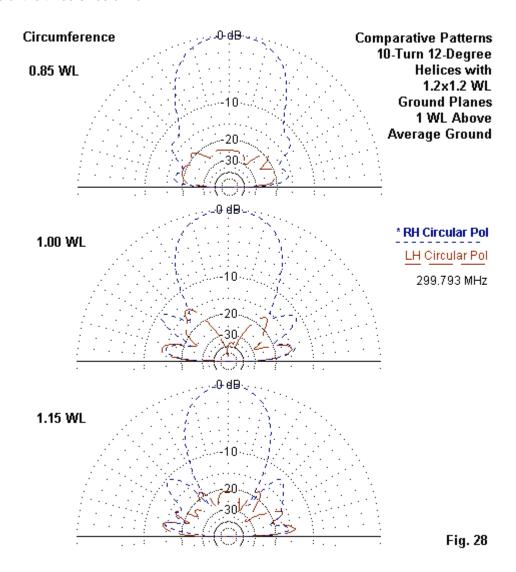
5-, 10-, 15-Turn Helices 1 WL Up
Reactance over Average Ground

Fig. 26

5 T-Ave Gnd   10 T-Ave Gnd   15 T-Ave Gnd

5-, 10-, 15-Turn Helices 1 WL Up
Reactance over Average Ground

Fig. 27

5 T-Ave Gnd   10 T-Ave Gnd   15 T-Ave Gnd

Fig. 26 and **Fig. 27** provide data for the elevated ground-plane models on the source resistance and reactance, respectively. The overlap in the curves for a good portion of their length suggests that--with one exception--they portray the source impedance trends quite well. The curves for circumferences above 0.90λ and those for 0.90λ and lower have slightly different slopes. 0.90λ is the last circumference using a 0.1λ grid-wire connection; from 0.95λ upward, the connection is to the 0.2λ grid wire junction.

The upper limit of source impedance stability is a circumference of about 1.15λ. At the lower end of the scale, the short (5-turn) helix deviates significantly below 0.8λ circumference. However, the other two sizes of helix appear to be stable to the limit of the survey. These results are consistent with the gain behaviors of the three sizes of helix.
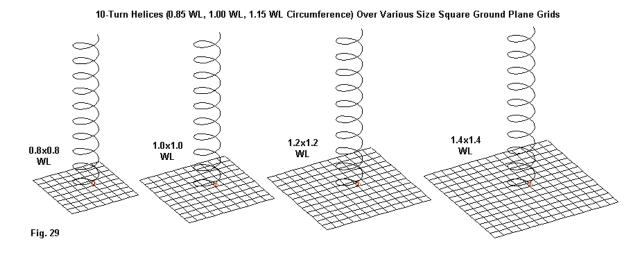

Fig. 28

The use of smaller circumferences for 12° helical antennas receives support from the evolution of patterns. **Fig. 28** presents a set of three patterns for the 10-turn model at 0.85λ, 1.0λ, and 1.15λ circumferences. EZNEC provides circularly polarized patterns, although the present set has maximum values that do not differ materially from a total-field pattern. All antennas in the series use right-hand circular polarization. Because reverse orientation pattern lobes occur in null areas of the dominant orientation, the total field patterns would show more complex structures in the region of the secondary lobes.

For most cases, the elevated ground-plane models show slightly less severe sidelobe strength, down from 1 to 1.5 dB relative to patterns for models over a perfect ground. Nevertheless, the sidelobe structure of the 1.15λ circumference model is sizable and peaks only about 10 dB below the main lobe of the pattern. In contrast, the 0.85λ circumference model has scarcely any sidelobe structure at all. However, pattern cleanliness will cost about 1 dB in maximum gain.

The end result of our survey of 12° helices over elevated ground planes is a set of data that differs in detail but not in main lines from the data for helices over perfect ground. Pressing for maximum gain by using a larger circumference results in a pattern with a much higher sidelobe content. As well, the helix may approach a region of unstable operation where small physical changes may yield large and unexpected changes in the source impedance. Leaning toward smaller circumferences sacrifices some gain for the sake of cleaner patterns and more predictable source impedance behavior.
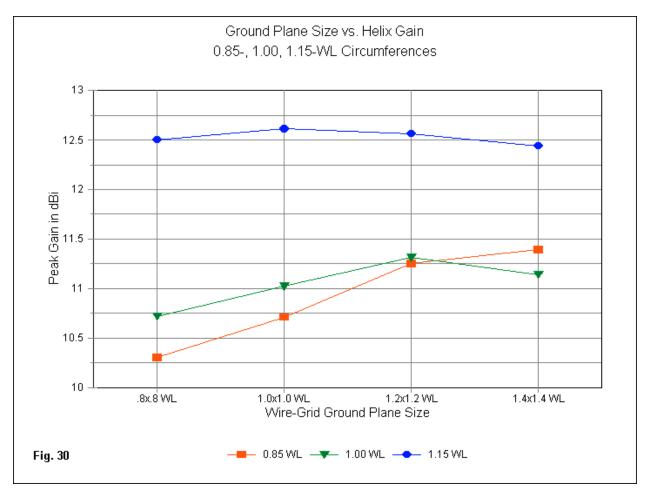
Is There a "Best" Ground Plane Size?

Within the context of square ground planes, the 1.2λ by 1.2λ wire grid used in the survey of 12° helices was both arbitrary and reasonable. I selected a size that I presumed was large enough to perform well in its function. However, without comparators, the ground plane that I used is not certifiably the best. To see if there might be a better size, I performed a final survey using 4 different square ground planes, with sides that are 0.8λ, 1.0λ, a.2λ, and 1.4λ long. **Fig 29** shows their relative sizes with respect to a standard helix.

10-Turn Helices (0.85 WL, 1.00 WL, 1.15 WL Circumference) Over Various Size Square Ground Plane Grids

Fig. 29

The ground planes all use 0.1λ wire spacing and 0.015λ wire diameters. This arrangement allows a standard relocation of the first wire in the helix. All first wires for 0.85λ circumference helices go to the 0.1λ position, while each of the two larger sizes (1.0λ and 1.15λ) move to the 0.2λ junction. A finer gradation of wire-grid sizes is desirable. However, such grids would create one or two problems. The use of standard 0.1λ wire spacing moves the first helix wire termination to a different position, creating deviations in the data and the AGT values. Creating a grid that places a wire at both the 0.1λ and 0.2λ position changes the performance of the grid for intermediate outside dimensions. Nevertheless, the 4 samples are enough to establish a basic trend.

Fig. 30 provides a view of the results of the sampling, while **Table 7** gives the complete tabular results. Although nothing significant happens in the realm of source impedance, the 10-turn helices used in the survey show small but definite differences in gain as we change the size of the ground plane. The larger the circumference of the helix, the smaller is the ground-plane size that yields maximum gain. Each of the three sizes of helix--as measured by circumference--has its peak gain with a different size ground plane. What the survey cannot show is whether the overall length of the helix plays a role in the ground-plane size for peak gain, since the smaller circumference models also have a shorter total length.

Fig. 30

The gain difference for the widest helix is not great across the span of ground-plane sizes. However, as we reduce the circumference of the helix, the curves grow steeper. Since the survey stops at a 1.4λ side length for the ground plane, it is not clear whether or not the 0.85λ circumference helix has reached its peak value. Still, ground-plane size is another of those factors that basic helix literature tends to overlook. The amateur who intends to build his own axial-mode helix should not ignore this factor. For the 0.85λ circumference helix, the gain difference between the smallest and largest ground planes in the series is over 1 dB.

Is the Helical Antenna the Best Choice for Amateur Radio Circularly Polarized Communications?

These notes have recorded some interesting limitations in the stability and the patterns of axial-mode helical antennas. Calculating the required helix dimensions turns out to be the simplest part of the planning process. Much more hangs upon the decisions we make with respect to selecting the circumference and ground plane sizes, as we weigh the contributing factors in a compromise between having the cleanest pattern, the most stable source impedance, and the maximum gain. A single set of dimensions may not satisfy all possible operating conditions.

Most engineering sources classify the axial-mode helical antenna as a broadband array. Within this classification, we expect limitations of the sort that we encountered. However, amateur communications calling for circular polarization generally require only narrow-band antennas. Before we close the notes, we should at least do a preliminary comparison of alternative antennas that an amateur might use in satellite communications.
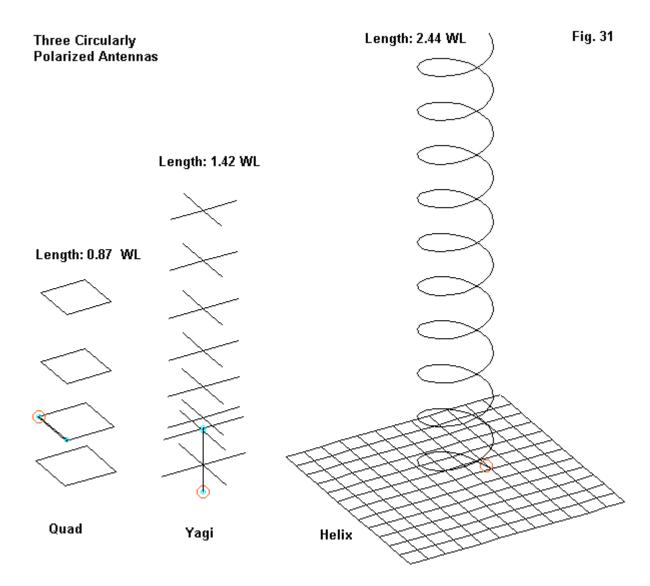
Three Circularly Polarized Antennas

Length: 2.44 WL

Fig. 31

Length: 1.42 WL

Length: 0.87 WL

Quad

Yagi

Helix

Fig. 31 presents the outlines of three antennas. All are designed for the test frequency of 299.7925 MHz. The helix, selected from the cluster that we have studied, uses 10 turns, 2-mm wire, and a 12° pitch. The 1.15λ circumference results in a total length of 2.44λ. To make the model coincide with the other antennas, I elevated the terminal end of the helix and created a 1.2λ by 1.2λ wire grid as an elevated ground plane. Other ground plane structures are possible. I experimented with 32- and 64-radial ground planes. However, the need to terminate the first segment of the helix at the center of the radial system established quickly that the helix must be almost perfectly centered over its ground plane structure. Off-setting the radial planes by less than 0.2λ reduced main lobe gain by 3 dB and produced a major secondary lobe only 4-5 dB weaker than the main lobe.

The helix over the square wire grid was centered, with only the first segment moved slightly (about 0.017λ) to intersect a grid-wire end. The gain (corrected for an AGT-dB value of -0.79 dB) was 12.77 dBi with a beamwidth of 37°. The impedance (corrected for an AGT of 0.859) was about 220Ω, although the impedance at the actual junction will be somewhat lower still.

The other two antennas in the set are a 4-element quad with a turnstiled driver and an 8-element crossed Yagi with turnstiled drivers. The quad is only 0.87λ long from reflector to the forward-most director. Using 1-mm diameter wire for the elements, it has a gain of 10.35 dBi when placed 1λ above average ground. The gain value is close to that of a 5-turn helix constructed like the 10-turn version just

shown. The quad's beamwidth is 58°. Because a quad allows some flexibility in the placement of the driver without undue adverse effects on the array gain, we may arrive at a single-source impedance of about 95Ω resistive. Hence, a 1/4λ section of 93Ω cable forms a proper phase line run between successive corners of the driver. The result is a circularly polarized antenna. We may reverse the polarization simply by connecting the main feedline at one or the other end of the phase line. The result is a 50-Ω impedance for the main feedline. The 4-element quad in the outline sketch has a 2:1 50Ω SWR bandwidth of more than 25 MHz, which eases the problems associated with construction variables. (Redesigning the antenna for fatter elements would yield a larger bandwidth.) Obviously, longer versions are possible for the quad if one desires more gain.
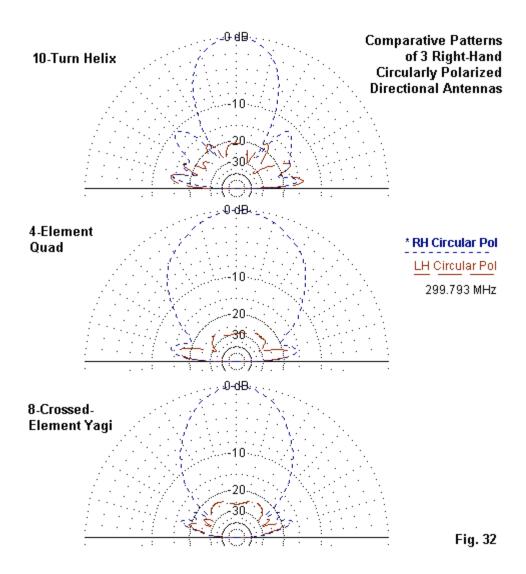
The 8-crossed-element Yagi is 1.42λ long, about 60% of the length of the sample helix. It uses half-inch (12.7-mm) elements. As the sketch shows, the parasitic elements meet at the center, although the drivers require a small separation to effect the turnstile feed. In this particular design, the single driver source impedance is 50Ω. Hence, the turnstile phase-line is also 50Ω. The resulting impedance presented to the main feedline is close to 25Ω. A length of 35Ω line (or a pair of 70Ω lines in parallel) provides the required match for a 50Ω main feedline. As with the quad, one may change polarization simply by swapping phase-line ends for the junction with the matching section and main feedline. To center the design frequency within the overall 2:1 50Ω SWR passband, the line lengths for both the phase line and the matching line are not true quarter-wavelengths electrically. The electrical length of the phase-line is a bit over 0.22λ, while the matching line is close to 0.215λ. The 2:1 SWR passband runs between 270 and 330 MHz, a 60-MHz spread that should make home construction less critical.

The Yagi produces a modeled 12.58 dBi gain when the antenna reflectors are 1λ above average ground. The gain is approximately the same as that of the much longer 10-turn helix. The modeled beamwidth is 44°. Compare these values to the shorter quad values of 10.35 dBi and 58°. Anyone interested in either type of antenna can make the appropriate comparisons that weigh performance differences against construction complexity. The Yagi and the helix are equivalent performers in terms of gain, while the shorter quad lags in performance while leading in simplicity. Regardless of the actual gain of each antenna in the field, we have another interest in the three antennas: the pattern shape and the sidelobe production.

The Yagi has a front-to-sidelobe ratio of about 16.6 dB. The corresponding ratio for the quad is about 14 dB. In contrast, the axial-mode helix has a front-to-sidelobe ratio of only 11.1 dB. Note the improvement of the sidelobe performance relative to the models over perfect ground. The elevated 10-turn helix shows a front-to-sidelobe ratio improvement of about 1.6 dB. Nevertheless, the helical antenna sidelobe structure bears watching. Equally important is the distribution of energy to the sides. For this purpose, I remodeled the helix (along with the quad and Yagi) in EZNEC Pro/4, since it provides pattern plots that distinguish the left-hand and right-hand circular polarization of any test antenna. **Fig. 32** shows the plots for the three sample antennas.

Both the Yagi and quad show diminutive side lobes at low angles. The total energy in these sidelobes, as measured by the area they occupy, is quite small. In contrast, the higher-angle lobes of the helix occupy a broad front on each side of the main lobe. Hence, their sensitivity to signals and noise not associated with the communications target is considerably higher than the comparable sensitivity of the parasitic arrays.

In addition to having smaller sidelobes, both the quad and the Yagi show less reverse polarization energy as well. (Reciprocally, transmitted energy becomes receiving sensitivity.) Once past the 4-element stage, quads tend to require more boom length for a given gain, due to the increased coupling at the corners. Hence, the proper "rival" for the helix is the crossed-element Yagi, and its gain-to-boom-length ratio is virtually identical to that of the helix. If the Yagi's smaller sidelobes make a difference to communications quality, then it might make a better choice than the helix. If switching polarization is necessary, then the Yagi and the quad have an advantage over the helix, with its permanent spiral. With respect to gain, none of the models in this sample comparison squeeze the last fraction of a dB from the designs. Because the aim of this final section is only to show alternatives to the helix and their potential relative performance, I have omitted quad and Yagi dimensions.

Fig. 32

Conclusion

I began this study because the available literature on axial-mode helical antennas seemed somewhat oblivious to matters other than the maximum potential gain. Pattern shape went largely ignored except in the context of a broadband antenna in the King and Wong treatment. Performance stability for the spot frequency applications that mark amateur use of these antennas also passed in relative silence. These notes have tried to focus on these aspects of helix performance by using a limited number of cases to establish some definite trends that apply to the home construction of axial-mode helices.

The net result has been to see that for most cases, it is unwise to try to derive the maximum gain of which a helix is capable by widening its base. Unstable source-impedance conditions and serious sidelobes develop before the antenna reaches the maximum gain size. In the end, a practical axial-mode helix has only the gain of a well-designed crossed-element Yagi of a similar boom length, and the Yagi tends to have smaller sidelobes and switchable polarization.

These results, of course, cannot contend with raw curiosity, which alone will lead many amateur antenna builders to construct helices. At most, these notes can temper enthusiasm with an appreciation of the limitations of the helix. It remains about the best high-gain broadband circularly polarized design available. However, to obtain the best from the design, one must attend to the costs and limits of the design as well as to its potentials.

* * * *

Note: Originally produced for the *Proceedings of the Southeastern VHF Society*, April, 2005.